BIOCHEMISTRY
including biophysical chemistry & molecular biology

Article

pubs.acs.org/biochemistry

Stereochemical Outcome at Four Stereogenic Centers during Conversion of Prephenate to Tetrahydrotyrosine by BacABGF in the Bacilysin Pathway

Jared B. Parker and Christopher T. Walsh*

Department of Biological Chemistry and Molecular Pharmacology, Harvard Medical School, 240 Longwood Avenue, Boston, Massachusetts 02115, United States

Supporting Information

ABSTRACT: The first four enzymes of the bacilysin antibiotic pathway, BacABGF, convert prephenate to a tetrahydrotyrosine (H_4Tyr) diastereomer on the way to the anticapsin warhead of the dipeptide antibiotic. BacB takes the BacA product *endocyclic*-Δ^4,Δ^8-7*R*-dihydrohydroxyphenylpyruvate (*en*-H_2HPP) and generates a mixture of 3*E*- and 3*Z*-olefins of the *exocyclic*-Δ^3,Δ^5-dihydrohydroxyphenylpyruvate (*ex*-H_2HPP). The NADH-utilizing BacG then catalyzes a conjugate reduction, adding a pro-*S* hydride equivalent to C_4 to yield tetrahydrohydroxyphenylpyruvate (H_4HPP), a transamination away (via BacF) from 2*S*-H_4Tyr. Incubations of the pathway enzymes in D_2O yield deuterium incorporation at C_8 from BacA and then C_9 from BacB action. By ^{1}H NMR analysis of samples of H_4Tyr, the stereochemistry at C_4, C_8, and C_9 can be assigned. BacG (followed by BacF) converts 3*E*-*ex*-H_2HPP to 2*S*,4*R*,7*R*-H_4Tyr. The 3*Z* isomer is instead reduced and transaminated to the opposite diastereomer at C_4, 2*S*,4*S*,7*R*-H_4Tyr. Given that bacilysin has the 2*S*,4*S* stereochemistry in its anticapsin moiety, it is likely that the 2*S*,4*S*-H_4Tyr is the diastereomer "on pathway". NMR determination of the stereochemistry of the CHD samples at C_8 and C_9 allows assignment of all stereogenic centers (except C_3) in this unusual tetrahydro-aromatic amino acid building block, giving insights into and constraints on the BacA, BacB, and BacG mechanisms.

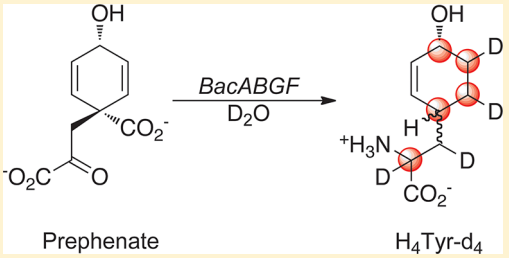

The dipeptide antibiotic bacilysin, produced by strains of *Bacillus subtilis*, consists of L-alanine in amide linkage with the nonproteinogenic amino acid anticapsin.[1] Anticapsin is 3-epoxycyclohexanonyl-alanine and bears the reactive epoxyketone warhead that covalently captures the active site cysteine thiolate in the glutaminase domain of the enzyme glucosamine-6-phosphate synthase.[2] Blockade of this enzyme shuts down production of GlcNAc units required for both bacterial and fungal cell wall assembly.[3,4] The producing *B. subtilis* ligates anticapsin to L-Ala to protect itself and then exports the resultant bacilysin as a prodrug. Uptake by a dipeptide permease transporter of a neighboring microbial cell followed by dipeptidase action liberates anticapsin in a neighboring victim cell (Figure 1).

The biosynthetic pathway to anticapsin, and then bacilysin, has been studied genetically to reveal a cluster of five *bacA*−*E* genes,[5,6] and more recently at the enzyme level to decipher the molecular logic for construction of the epoxycyclohexanone moiety of this unusual amino acid.[7] The biochemical studies have shown that *ywfGH*, the latter transcribed on the opposite DNA strand from *bacA*−*E*, encode an NADH-dependent reductase (*ywfH*) and an L-specific transaminase (*ywfG*) that carry out steps 3 and 4 of the pathway. Therefore, we rename the genes *bacF* (*ywfG*) and *bacG* (*ywfH*) and use that nomenclature throughout this work (Figure 2). In sum, the set of four enzymes BacABGF, in that order, act in tandem to divert some of the cellular flux of prephenate away from Phe and Tyr biosynthesis and into the anticapsin pathway, yielding tetrahydrotyrosine (H_4Tyr) as an intermediate.[7]

We have previously determined that BacA decarboxylates prephenate without aromatization[7] and in the process specifically isomerizes the pro-*R* double bond in the 1,4-diene system to yield *endocyclic*-Δ^4,Δ^8-7*R*-dihydrohydroxyphenylpyruvate (*en*-H_2HPP).[8] The next enzyme, BacB, conducts an allylic isomerization to move the double bond into conjugation at the exocyclic Δ^3-position (*ex*-H_2HPP). In so doing, it generates a 3/1 mixture of the *E*- and *Z*-geometric isomers at the Δ^3-olefin upon equilibration. The third enzyme, BacG, uses NADH to reduce that conjugated exocyclic double bond and yield an H_4HPP product.[7] The fourth enzyme, BacF, is a transaminase and uses L-Phe as an amino donor to reductively aminate the 2-keto group of H_4HPP and yields an H_4Tyr diastereomer (Figure 2).

The H_4Tyr is presumably two steps away, epoxidation of the olefin and oxidation of the C_7-OH group to the ketone, from anticapsin. H_4Tyr, an unusual noncanonical amino acid, has three stereocenters: C_2, C_4, and C_7. As shown below, BacF action, with L-Phe as the cosubstrate, sets the *S*-stereochemistry at C_2, and we have previously established[8] that BacA sets *R*-stereochemistry at C_7, which is carried through to H_4Tyr.

Received: May 16, 2012
Revised: June 21, 2012
Published: July 5, 2012

   dx.doi.org/10.1021/bi3006362 | *Biochemistry* 2012, 51, 5622−5632

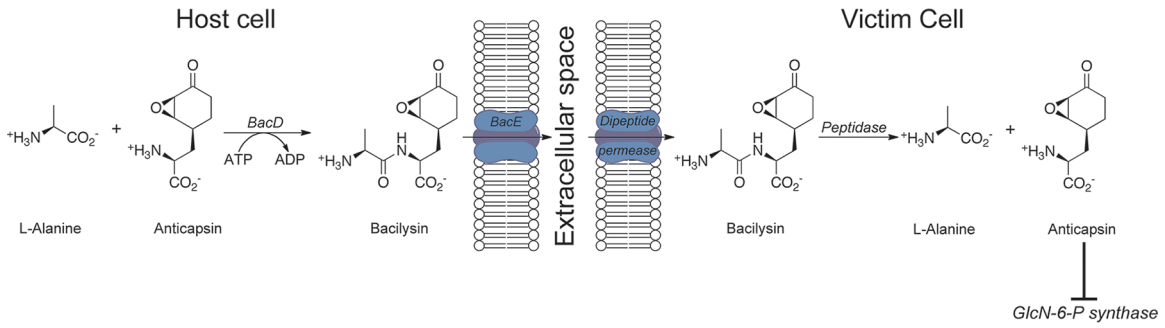

Figure 1. Ligation of L-alanine and anticapsin yields the dipeptide antibiotic bacilysin. The host cell further self-protects from anticapsin and bacilysin toxicity by transporting it into the extracellular environment, where it can be imported by neighboring cells. Peptide bond cleavage of bacilysin releases the anticapsin warhead, which blocks cell wall biosynthesis via inhibition of glucosamine-6-phosphate synthase.

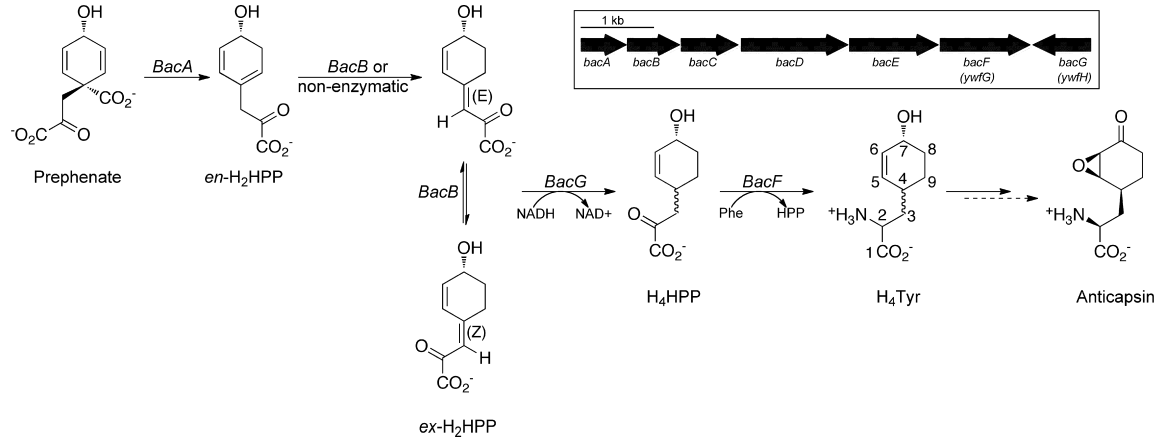

Figure 2. Proposed pathway for the biosynthesis of anticapsin from prephenate. YwfG and YwfH are hereby renamed BacF and BacG, respectively, as noted in the inset.

At issue then is the stereochemistry at C_4, presumably established by the NADH-utilizing BacG. Also of note is the fact that while the protio version of H_4Tyr has the three previously mentioned stereogenic centers, if the BacA, BacB, and BacG incubations starting from prephenate are conducted in D_2O buffers, then one deuterium (D = ^{2}H) is incorporated at C_8 via the action of BacA, one at C_9 from the action of BacB, and then another incorporated at C_3 by BacG catalysis (the hydride from NADH is added at C_4).[7] Thus, the C_3, C_8, and C_9 methylene groups (-CH_2-) become chiral by virtue of deuterium substitution (-CHD-). Therefore, in $^2H_3$-, $^2H_8$-, and $^2H_9$-containing samples, H_4Tyr produced via the BacABGF pathway possesses six chiral centers: C_2−C_4 and C_7−C_9. In this study, we report delineation of stereochemistry at the four centers (C_2, C_4, C_8, and C_9) that provide mechanistic insights and constraints into the action of BacF, BacG, BacA, and BacB, respectively.

MATERIALS AND METHODS

Materials and Instrumentation. Prephenic acid barium salt, L- and D-tyrosine (Tyr), L- and D-phenylalanine (Phe), 4-hydroxyphenylpyruvic acid (HPP), β-nicotinamide adenine dinucleotide hydrate (NAD^+), and β-nicotinamide adenine dinucleotide reduced disodium salt hydrate (NADH) were purchased from Sigma-Aldrich. NMR solvent (D_2O), D-glucose (1-D, 98%), and ethanol-d_6 (D, 99%) were purchased from Cambridge Isotope Laboratories. The enzymes glucose dehydrogenase from *Pseudomonas* sp., alcohol dehydrogenase from *Saccharomyces cerevisiae*, and aldehyde dehydrogenase from *S. cerevisiae* were also purchased from Sigma-Aldrich.

^{1}H and two-dimensional NMR spectra were recorded at 25 °C on a Varian VNMRS 600 MHz spectrometer equipped with a triple-resonance probe. ^{13}C one-dimensional NMR spectra were recorded on a Varian MR 400 MHz spectrometer (100.497 MHz for ^{13}C) equipped with a OneNMR probe. NMR data were analyzed and integrated with ACD/Laboratories software. High-resolution LC−MS data were collected on an Agilent Technologies 6520 Accurate-Mass Q-TOF LC−MS system and analyzed using its accompanying software. HPLC was performed on a Beckman Coulter System Gold instrument, and peaks were analyzed using the accompanying Karat 32 software. UV−vis measurements were collected using a Cary 50 BIO UV−vis spectrometer and analyzed with the accompanying software.

Cloning, Expression, and Purification of the Enzymes BacABGF. The cloning of plasmids for production of BacABGF has been previously described.[7] The expression and purification of BacA and BacB were also performed as previously described.[8] The expression and purification of BacG and BacF were identical to the procedure for BacA. Protein concentrations of BacABGF were determined by UV−vis absorbance using the following extinction coefficients (ε_{280}) calculated from the protein primary sequence using the ExPASy Bioinformatics Research Portal: 17420 M^{-1} cm^{-1} for BacA, 24410 M^{-1} cm^{-1} for BacB, 9970 M^{-1} cm^{-1} for BacG, and 41830 M^{-1} cm^{-1} for BacF.

Generation and Purification of Protonated 3*Z*-7*R*- and 3*E*-7*R*-*ex*-H_2HPP Isomers for Use as Substrates for NMR and Kinetic Analyses of BacG Action. Conversion of barium prephenate to potassium prephenate was performed as previously described.[7] Protonated 3*E*-*ex*-H_2HPP was generated

dx.doi.org/10.1021/bi3006362 | *Biochemistry* 2012, 51, 5622−5632

in reaction mixtures containing 12 mM potassium prephenate, 4 μM BacA, and 1 μM BacB in 2 mL of potassium phosphate buffer (pH 8.0). The reaction mixtures were incubated at ~20 °C for 16 h. The reactions were quenched via addition of acetonitrile to a concentration of 30% (v/v), and the mixtures were frozen and lyophilized in preparation for purification (discussed after generation of 3*Z*-*ex*-H_2HPP).

Production and purification of large amounts of 3*Z*-*ex*-H_2HPP from BacAB reactions were found to be very laborious because of a maximum of only 25% of the total product being the 3*Z* isomer.[8] However, NMR and kinetic experiments with the enzymes AerD and AerE (BacA and BacB homologues, respectively, from *Planktothrix agardhii*[9]) showed that these enzymes produce products identical to those of BacAB action when acting on prephenate substrate, except the 3*Z*/3*E* isomer ratio is 9/1 (J. B. Parker and C. T. Walsh, unpublished data) as opposed to 1/3 for BacAB. Thus, fully protonated 3*Z*-*ex*-H_2HPP was generated from AerDE reaction mixtures containing 12 mM potassium prephenate, 2 μM AerD, and 4 μM AerE in 4 mL of 50 mM potassium phosphate buffer (pH 8.0). {It is important to note that formation of the 3*Z* isomer from either AerE or BacB action was severely inhibited by high concentrations of salt [approximately >250 mM (data not shown)].} The reaction mixtures were incubated at ~20 °C for 16 h; the reactions were quenched via addition of acetonitrile to a final concentration of 30% (v/v), and the mixtures were frozen and lyophilized to dryness.

For purification of the *ex*-H_2HPP isomers, the lyophilized reaction mixtures of BacAB (for 3*E* isomer formation) and AerDE (for 3*Z* isomer formation) were resuspended (separately) in 750 μL of 10 mM potassium phosphate buffer (pH 8.0) and loaded onto a 100 mm × 21.2 mm Hypercarb column (Thermo Scientific) equilibrated in the resuspension buffer. Bound compounds were eluted (3*Z* and 3*E* isomers separated) by exposure to a shallow linear gradient of acetonitrile. Compound elution was monitored by UV absorbance at 295 nm. Fractions containing the appropriate isomers (normally ~30 mL) were pooled, frozen, and lyophilized to dryness. Pure *ex*-H_2HPP isomers were then moderately desalted by being resuspended in 500 μL of 10 mM potassium phosphate buffer (pH 8.0) and loaded onto a 100 mm × 10 mm Hypercarb column equilibrated in the same buffer. Bound *ex*-H_2HPP was eluted with a sharp linear gradient of acetonitrile (0 to 90% over 25 min), and 4.5 mL of fractions containing *ex*-H_2HPP were pooled and lyophilized to dryness. The lyophilized compound and residual potassium phosphate buffer were resuspended in 300 μL of ddH_2O, and the concentration was determined by UV−vis absorbance [ε_{295} = 15300 M^{-1} cm^{-1} for the 3*E* isomer,[7] and ε_{295} = 13700 M^{-1} cm^{-1} for the 3*Z* isomer (Figure S10 of the Supporting Information)]. Isomer purity was analyzed via analytical HPLC using a 100 mm × 2.1 mm Hypercarb column equilibrated in 10 mM potassium phosphate buffer (pH 8.0). Bound isomers were eluted using a linear gradient of acetonitrile, and elution was monitored by UV−vis absorbance at 295 nm (Figure S1 of the Supporting Information). Isomers were stored at −80 °C to prevent nonenzymatic isomer equilibration when not in use.

Kinetics of the Action of BacG on 3*Z*- and 3*E*-*ex*-H_2HPP. Kinetic reaction mixtures for the analysis of the action of BacG on 3*Z*-*ex*-H_2HPP contained 1 μM BacG, 2 mM NADH, 0−1.1 mM 3*Z*-*ex*-H_2HPP, and 50 mM potassium phosphate buffer (pH 8.0) in a volume of 250 μL. Kinetic reaction mixtures for the analysis of the action of BacG on 3*E*-*ex*-H_2HPP contained 5 μM BacG, 2 mM NADH, 0−8 mM 3*E*-*ex*-H_2HPP, and 50 mM potassium phosphate buffer (pH 8.0) in a volume of 250 μL. NADH (2 mM) was found to be >90% saturating for the reactions of both isomers. Reactions were initiated via addition of BacG, and the progress of the reaction was monitored by observing the oxidation of NADH to NAD^+ (UV absorbance at 370 nm) in a 1 mm cuvette. Reaction velocities (k_{obs}) in units of absorbance per minute were determined by calculating the slope of the initial, linear region of the 370 nm time course of each reaction. The change in NADH absorbance at 370 nm was converted to concentration using the experimentally determined extinction coefficient ε_{370} of 2690 M^{-1} cm^{-1} (referenced to NADH concentration determined from the ε_{340} of 6220 M^{-1} cm^{-1} [10]). Data were fit to the Michaelis−Menten equation (eq 1) using GraphPad Prism

$$k_{obs} = \frac{k_{cat}[S]}{K_m + [S]} \quad (1)$$

where k_{cat} is the maximal velocity, [S] is the substrate concentration, and K_m is the substrate concentration that yields $k_{obs} = {}^1/_2 k_{cat}$.

All reactions were performed in triplicate except the reaction that contained 8 mM 3*E*-*ex*-H_2HPP, which was performed in duplicate because of a lack of material.

Generation and Purification of Protonated 4*S*- and 4*R*-H_4HPP and 4*S*- and 4*R*-H_4Tyr Isomers for NMR Analysis. 4*S*-H_4HPP was generated in a reaction mixture containing 2 mM 3*Z*-*ex*-H_2HPP, 5 mM NADH, and 20 μM BacG incubated in 1 mL of 50 mM potassium phosphate buffer (pH 8.0). 4*S*-H_4Tyr was generated in a reaction mixture containing ~2 mM 4*S*-H_4HPP (described in the previous sentence), 10 mM L-Phe, 0.1 mM PLP, and 20 μM BacF in 1 mL of 50 mM potassium phosphate buffer (pH 8.0). 4*R*-H_4HPP was generated in a reaction mixture containing 2 mM 3*E*-*ex*-H_2HPP, 5 mM NADH, and 20 μM BacG in 1 mL of 50 mM potassium phosphate buffer (pH 8.0). 4*R*-H_4Tyr was generated in a reaction mixture containing ~2 mM 4*R*-H_4HPP (described in the previous sentence), 10 mM L-Phe, 0.1 mM PLP, and 20 μM BacF in 1 mL of 50 mM potassium phosphate buffer (pH 8.0). All reaction mixtures were incubated at ~20 °C for 16 h.

All of the reactions described above were quenched via addition of acetonitrile to a final concentration of 30% (v/v), and the mixtures were frozen and lyophilized to dryness. Dried reaction mixtures were resuspended in 500 μL of 10 mM potassium phosphate buffer (pH 8.0) and purified as described above for the *ex*-H_2HPP isomers except using a 100 mm × 10 mm Hypercarb column. As H_4HPP and H_4Tyr do not have a characteristic UV−vis absorbance, their elution was monitored via LC−MS in negative detection mode (0.1% NH_4OH as the solvent additive) using a 50 mm × 2.1 mm Hypercarb column with ddH_2O as the mobile phase and acetonitrile as the eluent. A mass of 183.0668 was observed for the H_4HPP isomers (calcd, 183.0663) and 184.0986 (calcd, 184.0979) for the H_4Tyr isomers. Three milliliters of fractions containing the desired product were frozen and lyophilized to dryness, resuspended in 300 μL of 99.99% D_2O, and placed in a 5 mm D_2O matched Shigemi tube for NMR analysis.

NMR spectral assignments were made via analyses of ^1H, ^{13}C, ^1H−^1H gCOSY, ^1H−^{13}C gHSQC, ^1H−^{13}C gHMBC, and ^1H−^1H NOESY (500 ms mixing time) spectra. Proton spectra were referenced to residual H_2O (4.79 ppm), while ^{13}C spectra were referenced to the methyl carbon of acetonitrile (1.47 ppm).[11] [Acetonitrile was spiked into the NMR sample at 0.3%

dx.doi.org/10.1021/bi3006362 | *Biochemistry* 2012, 51, 5622−5632

(v/v) after all necessary spectra had been acquired, and an additional ^{13}C experiment was performed to obtain the reference so as not to contaminate the original spectra with the acetonitrile signal.] Unless otherwise stated, water suppression (via presaturation) was utilized in all proton spectra that were collected.

Generation and Purification of Deuterated 3*Z*-*ex*-H_2HPP and 3*E*-*ex*-H_2HPP from the Action of BacA and BacB and Deuterated 3*E*-*ex*-H_2HPP from the Action of Only BacA. The reaction mixtures for the production of deuterated *ex*-H_2HPP isomers from the action of BacAB contained 5 mM prephenate, 10 μM BacA, and 40 μM BacB in 1 mL of 95% D_2O containing 50 mM potassium phosphate (pD 8.0). The reaction mixtures were incubated at 37 °C for 24 h; the reactions were quenched, and the mixtures were purified and desalted as described above for the protonated *ex*-H_2HPP isomers. (BacAB reactions in D_2O were very inefficient at producing 3*Z*-*ex*-H_2HPP. Therefore, it took many of these reactions to obtain enough deuterated compound for NMR analysis.) After desalting and lyophilization, the purified deuterated 3*Z*- and 3*E*-*ex*-H_2HPP isomers were resuspended in D_2O, and ^1H, $^1H-^{13}C$ gHSQC, and $^1H-^1H$ NOESY data were collected and referenced as described above for the protonated H_4HPP isomers.

Production of deuterated 3*E*-*ex*-H_2HPP from BacA action (without BacB) in tandem with nonenzymatic diene isomerization was accomplished in a reaction mixture containing 10 mM prephenate and 10 μM BacA in 2 mL of 98% D_2O containing 50 mM potassium phosphate buffer (pD 8.0). The reaction mixture was incubated at 37 °C for 144 h. The progress of the extremely lethargic nonenzymatic isomerization in D_2O was monitored by UV absorbance (λ_{max} of *en*-H_2HPP = 258 nm; λ_{max} of *ex*-H_2HPP = 295 nm[7]). The reaction was then quenched; the mixture was purified and desalted, and ^1H and $^1H-^{13}C$ gHSQC NMR data were collected as described above for the BacAB-generated deuterated *ex*-H_2HPP isomers.

Enzymatic Synthesis of Deuterated H_4HPP Isomers and H_4Tyr Isomers in D_2O Solvent. Two forms of deuterated 4*R*-H_4HPP were produced in two distinct reactions. The first reaction mixture contained 1 mM deuterated 3*E*-*ex*-H_2HPP produced from the deuterated BacAB reaction (described above), 4 mM NADH, and 30 μM BacG in 1 mL of 97% D_2O containing 50 mM potassium phosphate buffer (pD 8.0). The second reaction mixture contained 5 mM potassium prephenate and 20 mM NADH and was simultaneously incubated with 20 μM BacABG in 95% D_2O containing 50 mM potassium phosphate buffer (pD 8.0). Likewise, two forms of deuterated 4*R*-H_4Tyr were produced in two distinct reactions. The first reaction mixture contained 2 mM deuterated 3*E*-*ex*-H_2HPP produced from BacAB action (described above), 8 mM NADH, 0.1 mM PLP, 10 mM L-Phe, and 15 μM BacGF in 1 mL of 97% D_2O containing 50 mM potassium phosphate buffer (pD 8.0). The second reaction mixture contained 5 mM potassium prephenate, 20 mM NADH, 20 mM L-Phe, 0.1 mM PLP, and 15 μM BacABGF in 95% D_2O containing 50 mM potassium phosphate buffer (pD 8.0).

Only one form of deuterated 4*S*-H_4HPP and 4*S*-H_4Tyr could be produced. The reactions for the production of deuterated 4*S*-H_4HPP and 4*S*-H_4Tyr were identical to the first set of reactions used to produce deuterated 4*R*-H_4HPP and 4*R*-H_4Tyr (described in the previous paragraph) except that deuterated 3*Z*-*ex*-H_2HPP (produced from the deuterated BacAB reaction described above) was used in place of 3*E*-*ex*-H_2HPP.

All deuterated H_4HPP and H_4Tyr production reaction mixtures were incubated at ∼20 °C for 16 h and then reactions quenched and mixtures purified; appropriate fractions were identified by LC−MS as for the protonated H_4HPP and H_4Tyr reactions described above. H_4HPP masses obtained were 185.0816, 186.0876, 187.0938, and 188.0993 (calcd, 185.0788, 186.0851, 187.0914, and 188.0977). H_4Tyr masses obtained were 186.1159, 187.1215, 188.1279, and 189.1339 (calcd, 186.1105, 187.1167, 188.1230, 189.1293). These masses correspond to compounds with incorporation of two, three, four, and five deuteriums, respectively.

Enzymatic Synthesis of 4*R*-^{2}H- and 4*S*-^{2}H-NADH. 4*R*-^{2}H-NADH (also known as A-side NADD) was synthesized following a modified protocol of Viola et al.[12] Ethanol-d_6 (25 mM), 10 mM NAD^+, 300 units of alcohol dehydrogenase, and 32 units of aldehyde dehydrogenase were mixed in 10 mL of 25 mM Taps buffer (pH 9.0). The pH of the buffer was readjusted to 9.0 after addition of the NAD^+ but before addition of enzymes. The reaction mixture was incubated at ∼20 °C, and reaction progress was monitored by following the appearance of NADH (UV absorbance at 340 nm). After the mixture had been incubated for 45 min, the reaction was quenched via protein removal using a 3500 MWCO centrifugal filtration device (Amicon).

4*S*-^{2}H-NADH (also known as B-side NADD) was synthesized according to a slightly modified protocol of Ottolina et al.[13] Glucose-d_1 (30 mM), 15 mM NAD^+, and 100 units of glucose dehydrogenase were mixed in 6 mL of 50 mM potassium phosphate buffer (pH 7.5). The pH of the buffer was readjusted to 7.5 before enzyme addition. Reaction progress was monitored, and the reaction was quenched (after an 80 min reaction time) exactly as for the A-side NADD synthesis reaction described above.

The processing of both NADD reactions was identical for the remaining steps. The postfiltration flow-through containing the NADD was frozen and lyophilized to dryness. The dried reaction components were resuspended in 1 mL of H_2O. NADD at this stage was used directly in the BacG enzymatic reactions after the pH had been corrected to 8.0. The NADD concentration was determined by UV absorbance (ε_{340} = 6220 M^{-1} cm^{-1} [10]). To prepare NADD samples for NMR analysis of the deuterium content at C_4, NADD was crudely purified by being loaded onto a 250 mm × 10 mm Luna C_{18} 5 μm HPLC column (Phenomenex) equilibrated in H_2O and 0.01% NH_4OH. Bound NADD was eluted using a linear gradient of acetonitrile spiked with 0.01% NH_4OH. Fractions containing NADD were identified by the characteristic absorbance maxima at 260 and 340 nm. The observed 260 nm/340 nm ratio was 2.3 for A-side and 2.5 for B-side NADD (previously reported as ∼2.2 − 2.3 for pure NADH[12]). Fractions containing NADD were pooled and lyophilized to dryness. Samples (2 mM) of both A-side and B-side NADD were prepared in 99.99% D_2O and placed in 5 mm D_2O matched Shigemi tubes for ^1H NMR analysis (Figure S2 of the Supporting Information). Pro-*R* and pro-*S* hydride peaks were identified on the basis of previous assignments.[13,14]

Enzymatic Synthesis of H_4HPP Isomers from BacG Action with 4*R*-^{2}H-NADH and 4*S*-^{2}H-NADH as Cosubstrates. Reaction mixtures for the generation of 4*S*- and 4*R*-H_4HPP from protonated 3*Z*- and 3*E*-*ex*-H_2HPP, respectively, contained 1 mM *ex*-H_2HPP, 2 mM ^{2}H-NADH, and 30 μM BacG in 1 mL of H_2O containing 50 mM potassium phosphate buffer (pH 8.0). The reaction mixtures were incubated, the reactions quenched, the mixtures purified, and the fractions identified exactly as described above for protonated H_4HPP isomers

dx.doi.org/10.1021/bi3006362 | *Biochemistry* 2012, 51, 5622−5632

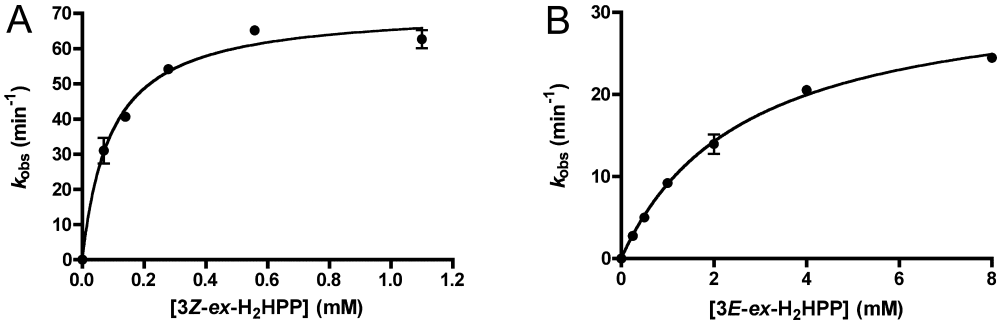

Figure 3. Michaelis–Menten kinetic traces for the reductase action of BacG on (A) 3*Z*-*ex*-H_2HPP (k_{cat} = 71.3 min^{-1}; K_m = 0.09 mM) and (B) 3*E*-*ex*-H_2HPP (k_{cat} = 33.2 min^{-1}; K_m = 2.7 mM) in the presence of a saturating level of NADH (2 mM).

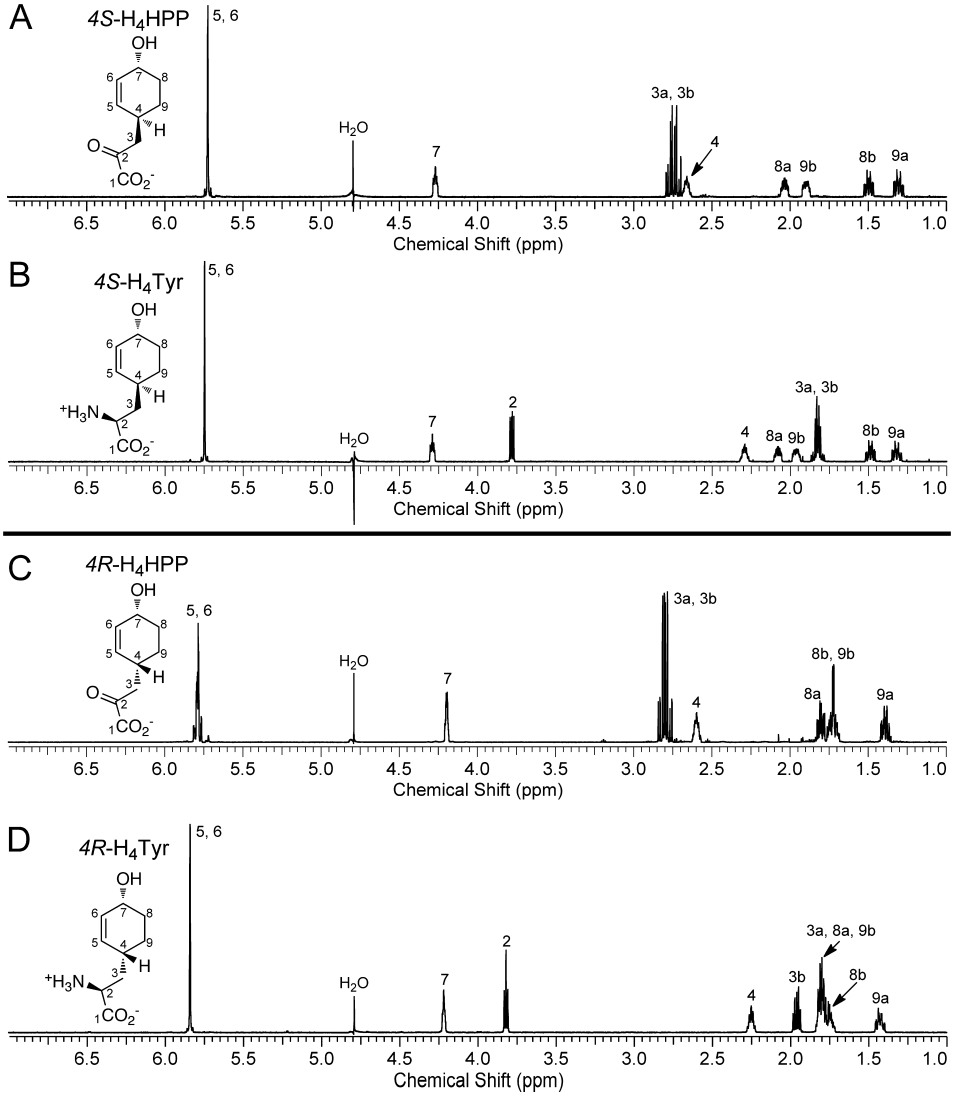

Figure 4. ^{1}H NMR traces of purified (A) 4*S*-H_4HPP from the action of BacG on 3*Z*-*ex*-H_2HPP, (B) 4*S*-H_4Tyr from the action of BacF on panel A, (C) 4*R*-H_4HPP from the action of BacG on 3*E*-*ex*-H_2HPP, and (D) 4*R*-H_4Tyr from the action of BacF on panel C.

generated from protonated NADH. The detected LC–MS mass of H_4HPP produced from 4*R*-^{2}H-NADH was 183.0670 (calcd, 183.0663). A major mass (184.0726) and a minor mass (183.0666) were both detected from H_4HPP produced from 4*S*-^{2}H-NADH (calcd, 184.0726 and 183.0663, respectively). Collection of ^{1}H and ^{1}H–^{13}C gHSQC NMR data was also performed as described above (Figure S3 of the Supporting Information).

Preparation of Tyrosine from the Transaminase Action of BacF on 4-Hydroxyphenylpyruvate for the Determination of Amino Acid Chirality. HPP (2 mM), 10 mM Phe (both L and D enantiomers in separate reactions), 0.5 mM PLP, and 10 μM BacF were mixed in 1 mL of 50 mM potassium phosphate buffer (pH 8.0). Reaction mixtures were incubated at ~20 °C for 16 h, reactions quenched via addition of acetonitrile to a final concentration of 30% (v/v), and mixtures lyophilized to

dx.doi.org/10.1021/bi3006362 | *Biochemistry* 2012, 51, 5622–5632

dryness and resuspended in 500 μL of H_2O. The expected transamination product (tyrosine) was identified from the BacF reaction mixture containing L-Phe by LC−MS in positive detection mode (0.1% formic acid as a solvent additive) using a 50 mm × 2.1 mm Hypercarb column with water as the mobile phase and acetonitrile as the eluent. No tyrosine was observed from the BacF reaction mixture containing D-Phe as the cosubstrate.

Prior to chiral HPLC analysis of the BacF-produced tyrosine, it was necessary to purify the nascent tyrosine from the other reaction components to avoid spectral contamination. The resuspended reaction mixture was loaded onto a 100 mm × 10 mm Hypercarb column equilibrated in 10 mM potassium phosphate buffer (pH 8.0). Bound compounds were eluted via a linearly increasing gradient of acetonitrile. Fractions containing tyrosine were initially located by their UV−vis spectra and later confirmed by LC−MS analysis as described above. The appropriate fractions were pooled and lyophilized to dryness. The amino acid chirality of the BacF-generated tyrosine was determined by comparing its elution profile from a 150 mm × 4.6 mm Chirex 3126 column (Phenomenex) equilibrated in 2 mM copper(II) sulfate in an 84/16 (v/v) water/methanol mixture with that of authentic L- and D-tyrosine standards. Tyrosine elution was monitored by UV−vis absorbance at 280 nm (Figure S4 of the Supporting Information).

RESULTS

BacG Acts on 3*Z*,7*R*- and 3*E*,7*R*-*ex*-H_2HPP Geometric Isomers To Give H_4HPP Products That Are Diastereomeric at C_4. In initial studies of the Bac pathway enzymes for the conversion of prephenate to H_4Tyr, we conducted incubations of either BacAGF or BacABGF in parallel, based on the observation that the BacA-derived *en*-H_2HPP will isomerize nonenzymatically and quantitatively into conjugation to give the exocyclic *ex*-H_2HPP product.[7] BacB accelerates the allylic isomerization by up to 10^3 and so was of use in shortening the kinetics in the four enzyme incubations.[15] These incubations could be conducted in buffered H_2O or buffered D_2O, to yield H_4Tyr with one deuterium each at C_8 and C_9 [as well as at C_2 and C_3 (vide infra)]. A deeper analysis of the BacB-mediated isomerization recently led us to the finding that while the *E*/*Z* ratio of *ex*-H_2HPP from BacA followed by nonenzymatic allylic isomerization was 50/1, in BacB-containing equilibrated incubations the *E*/*Z* ratio was 3/1. In turn, that led us to separation and structural assignment of the 3*E* and 3*Z* isomers on Hypercarb HPLC columns and a proposed mechanism for geometric isomer equilibration via dienolate intermediates.[8]

The presumption from the above results was that each of the 3*E*- and 3*Z*,7*R*-*ex*-H_2HPP geometric isomers could be a substrate for the NADH-utilizing BacG. This enzyme is assayed by loss of the 340 nm chromophore of the reduced nicotinamide ring of NADH as *ex*-H_2HPP is reduced to H_4HPP (and NADH is oxidized to NAD^+). Because of the partially overlapping chromophores of the *ex*-H_2HPP substrate (λ_{max} = 295 nm) and cosubstrate NADH, measurements of the reaction were taken away from the absorbance maximum of NADH, at 370 nm, where a sufficient signal-to-noise ratio persisted. Indeed, the separated geometric 3*E* (96% purity) and 3*Z* [97% purity (Figure S1 of the Supporting Information)] isomers were each saturable substrates (Figure 3). The k_{cat} for the 3*Z* isomer at 71.3 min^{-1} was approximately twice that for the 3*E* isomer (33.2 min^{-1}). The 3*Z* isomer also had a 30-fold lower K_m value (0.09 mM vs 2.7 mM). By k_{cat}/K_m ratios, which compare the relative catalytic efficiencies of two substrates for the same enzyme, the 3*Z*,7*R*-*ex*-H_2HPP isomer is a 64-fold better substrate than the corresponding *E* isomer. Thus, although the 3*Z* geometric isomer is kinetically disfavored during BacB action, and essentially absent from the nonenzymatic isomerization of *en*-H_2HPP to the thermodynamically favored *ex*-H_2HPP,[8] it is very much the preferred substrate for the conjugate reduction reaction of BacG.

Panels A and C of Figure 4 show the proton NMR spectra of the H_4HPP samples generated from the action of BacG on 3*Z*-*ex*-H_2HPP and 3*E*-*ex*-H_2HPP substrates, respectively. It is clear from examination of the H_8 and H_9 resonances that the products are distinct, most likely because of distinct diastereomers at C_4, the anticipated site of hydride addition by BacG. On subsequent BacF-mediated transamination of each of the H_4HPP keto acid samples to the corresponding 2*S*-H_4Tyr samples, the proton NMR spectra in panels B (derived from the Figure 4A sample) and D (derived from the Figure 4C sample) of Figure 4 also gave distinct diastereomers as evidenced by the distinct splitting patterns from the methylene hydrogens at C_3, C_8, and C_9. The assignments of the indicated stereochemistries as 4*S* (from the 3*Z* substrate) and 4*R* (from the 3*E* substrate) are detailed in a subsequent section.

Proof that BacG acted by conjugate addition of an NADH-derived hydride to C_4 of the *ex*-H_2HPP substrates was explicitly tested with 4*R*-D_1-NADH and 4*S*-D_1-NADH samples as reductants. ^{1}H NMR analysis of the two chirally deuterated NADH samples established that 4*R*-D_1-NADH was 40% D_1 while 4*S*-D_1-NADH was 62% D_1 (Figure S2 of the Supporting Information).

NMR analysis of the H_4HPP products from 4*R*-D_1-NADH incubations on both the 3*E*- and 3*Z*-*ex*-H_2HPP substrates shows the transfer of the diastereotopic 4-pro-*S* hydride to both the 3*E* and 3*Z* substrate isomers. Figure S3 of the Supporting Information shows the 3*Z* substrate had 0.94 equiv of ^{1}H at C_4 while the 3*E* substrate possessed 1.0 equiv of ^{1}H, referenced to the single hydrogen at C_7 in the product H_4HPPs. One could worry that the lack of deuterium reflected a kinetic isotope effect between NADH and 4*R*-D_1-NADH molecules in the NADH reductant pool, but the complementary results with the transfer of deuteride from the 4*S*-D_1-NADH sample ruled out that possible ambiguity. The 4*S*-D_1-NADH donor sample (62% deuterium content) gave H_4HPP with 68% D at C_4 when the 3*Z* substrate was reduced and 58% D at C_4 when the 3*E* substrate was reduced. These results clearly indicate that BacG transfers the pro-*S* hydride of NADH during *ex*-H_2HPP reduction.

These results validate several points. First, BacG is acting as a regiospecific hydride transfer catalyst to C_4 for each of the 3*E*- and 3*Z*-*ex*-H_2HPP substrate isomers. Second, the pro-*S* hydride of NADH is transferred to each of the substrate geometric isomers. Third, from the NMR spectra in panels A and C of Figure 4 noted above, the H_4HPP products are likely to be diastereomers at C_4.

The BacF Transaminase Is 2*S*-Specific. Given that the BacF transaminase processes L-Phe (2*S*) as an amino donor to cosubstrate H_4HPP, we anticipated it would show the same specificity toward partner keto acids that become reductively aminated. To that end, we have now demonstrated that while L-Phe is an effective amino donor, D-Phe is not (data not shown). To validate that the keto acid partner undergoing amination gives a 2*S* amino acid product, we used *p*-hydroxyphenylpyruvate as the acceptor with L-Phe as a donor. As anticipated, tyrosine was generated (LC−MS mass of 182.0805; calcd, 182.0812) as L-Phe

dx.doi.org/10.1021/bi3006362 | *Biochemistry* 2012, 51, 5622−5632

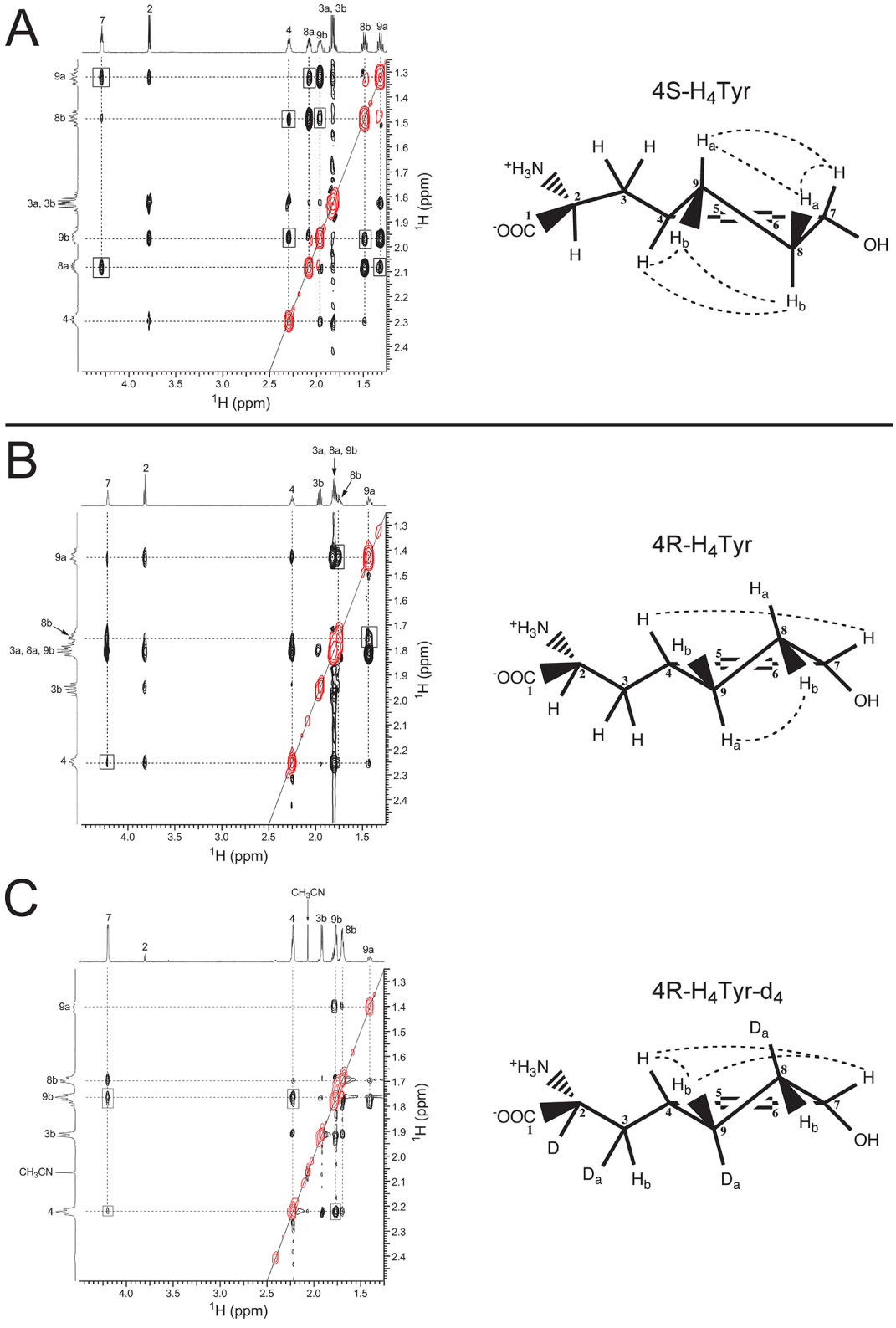

Figure 5. ^{1}H−^{1}H NOESY spectra and accompanying NOE correlations used to determine the C_4 stereochemistry of (A) 4*S*-H_4Tyr and (B) 4*R*-H_4Tyr. Because of the spectral overlap of H_{3a}, H_{8a}, and H_{9b} in the spectra of (B) 4*R*-H_4Tyr, NOE correlations of (C) 4*R*-H_4Tyr-d_4 were also analyzed to allow analysis of correlations to and from H_{9b} to complete the stereochemical determination. Black cross-peaks in the NOESY spectra indicate positive resonances, while red cross-peaks indicate negative resonances. Key NOE interactions have been noted on the structures with dashed lines, and the correlating cross-peaks are boxed in the NOESY spectra.

was oxidatively deaminated in the first half of the BacF reaction. The chirality of the nascent Tyr was determined to be "L" (2*S*) by comparison with authentic D- and L-Tyr samples by chiral HPLC (Figure S4 of the Supporting Information). By analogy, we assign the H_4Tyr from reductive amination of H_4HPP by BacF as the 2*S* diastereomer. At this point, with the 2*S* stereochemistry assigned,

dx.doi.org/10.1021/bi3006362 | *Biochemistry* 2012, 51, 5622−5632

we turned to analysis of the absolute stereochemistry at C_4 of the H_4Tyr samples generated from tandem action of BacABGF to obtain the absolute stereochemistry of the H_4Tyr emerging from the four enzymes in the bacilysin pathway.

Interpretation of NOE Correlations in Determining the Stereochemistry of 4*S*-H_4Tyr and 4*R*-H_4Tyr at C_4. To determine the stereochemistry at C_4 of H_4Tyr (and by inference H_4HPP) derived from BacG reduction of 3*Z*-*ex*-H_2HPP, we collected ^{1}H−^{1}H NOESY data reporting on the relative distances between protons on a fully protonated sample of H_4Tyr (Figure 5A). Because the proton resonances needed to make the appropriate correlations did not overlap in this sample, stereochemical assignment was straightforward. We began linking correlations using H_7 as the reference, because the stereochemistry at C_7 had been previously assigned in our earlier study as *R* stereochemistry.[8] From inspection of the NOE cross-peaks, it is seen that H_7 shows a strong correlation with H_{8a} and H_{9a}, but not H_{8b} and H_{9b}. This indicates that H_7, H_{8a}, and H_{9a} are on the same face of the cyclohexenol ring, while H_{8b} and H_{9b} are on the opposite face (Figure 5A). We then moved our attention to the H_4 proton and noticed that H_4 correlates strongly with H_{8b} and H_{9b}, but not H_{8a} and H_{9a}, indicating that H_4, H_{8b}, and H_{9b} are on the same face of the cyclohexenol ring and thus on the opposite face from H_7. These correlations establish that H_4Tyr (and thus H_4HPP, as shown in Figure 4) originating from BacG reduction of 3*Z*-*ex*-H_2HPP possesses 4*S* stereochemistry (Figure 5A).

Determination of the C_4 stereochemistry of H_4Tyr (and H_4HPP) derived from BacG reduction of 3*E*-*ex*-H_2HPP was not so straightforward because of the overlapping cross-peaks of H_{3a}, H_{8a}, and H_{9b} in the ^{1}H−^{1}H NOESY data of protonated H_4Tyr (Figure 5B). However, two important NOE correlations could be clearly seen in these data: a strong cross-peak between H_{8b} and H_{9a} and a weak cross-peak between H_4 and H_7. While the strong cross-peak between H_{8b} and H_{9a} indicates they are most likely on the same face of the cyclohexenol ring, the NOE correlation between H_4 and H_7 confirms that H_4 and H_7 are on the same face of the ring. This shows that 4*R*-H_4Tyr (and thus 4*R*-H_4HPP) is derived from the action of BacG on 3*E*-*ex*-H_2HPP (Figure 5B).

Although the stereochemistry at C_4 of 4*R*-H_4Tyr could be interpreted despite the overlapped resonances in the ^{1}H−^{1}H NOESY spectrum (Figure 5B), NOE analysis of 4*R*-H_4Tyr-d_4 (Figure 5C) was necessary to determine the relative positions of the nonequivalent protons of C_8 and C_9. As observed in Figure 5C and in greater detail in Figure S5B of the Supporting Information, simultaneous incubation of BacABGF with prephenate in 95% D_2O solvent incorporates one deuterium each at C_2, C_3, C_8, and C_9 of 4*R*-H_4Tyr-d_4 and fortuitously yields a ^{1}H NMR spectra without overlapped resonances. Inspection of the ^{1}H−^{1}H NOESY data of 4*R*-H_4Tyr-d_4 shows an especially strong cross-peak between H_4 and H_{9b}, indicating they are on the same face of the cyclohexenol ring. (For comparison, the cross-peak between H_4 and H_{9a} in Figure 5B is weaker. The cross-peak between H_4 and H_7 in panels B and C of Figure 5 can be used to normalize the spectra to each other.) Also in Figure 5C, almost equivalent cross-peak intensities are seen between H_7 and H_{8b} and between H_7 and H_{9b}. For this to be possible, H_{8b} would need to be on the opposite face of H_7 while H_{9b} would need to be on the same face as H_7. This correlation agrees with the determination made above that H_4 and H_{9b} are on the same face of the cyclohexenol ring (Figure 5C). Combined, these determinations imply that H_4, H_7, H_{8a}, and H_{9b} are on one ring face while H_{8b} and H_{9a} are on the opposing face (as suggested in Figure 5B by the strong correlation between H_{8b} and H_{9a}). Additional support for these analyses comes from the ^{1}H−^{1}H NOESY spectra of protonated 4*R*-H_4HPP spectra (Figure S9 of the Supporting Information), where H_{8a} is a distinct resonance. In this spectrum, strong correlations are seen between H_{8a} and the protons on C_4 and C_7 (same face) while little or no correlations are seen between H_{9a} and either H_4 or H_7 (opposite face).

Stereochemical Insights at C_8 and C_9 in Deuterated Samples of H_4HPP and H_4Tyr. A bonus from NMR analyses of the deuterated 4*R*- and 4*S*-H_4Tyr samples (as seen in Figure 5C and Figures S5B, S6C, and S7C of the Supporting Information) is information about the placement of deuterium at C_8 (from BacA action) and C_9 (from BacB action). We know the stereochemistry at C_2 is 2*S* from BacF transaminase action data cited above. We have not tried to determine the stereochemistry at the C_3-HD center. One deuterium is picked up at that site during BacG action, but there is also solvent exchange at C_3 when BacB conducts the equilibration between the 3*E* and 3*Z* isomers of *ex*-H_2HPP, via dienolate intermediates.[8] The extent of that exchange may well have differed during different incubations, leading to partial deuterium incorporations at C_3.

At C_8, the deuterium in both the 4*R*- and 4*S*-H_4Tyr products is on the same face as H_7; therefore, the stereochemistry in the C_8-HD samples is 8*S*. The stereochemical outcome at C_9 in the C_9-HD samples is more complex. As shown in Figure 5 and Figure S5B of the Supporting Information in the 4*R*-H_4Tyr sample from simultaneous BacABGF D_2O incubations with prephenate, the deuterium at C_9 is on the ring face opposite both H_4 and H_7 and therefore is the 9*S* monodeutero isomer.

The results with 4*S*-H_4Tyr samples from D_2O incubations were less clear-cut. Under some conditions (Figure S7C of the Supporting Information), with BacB present, there was partial deuterium substitution at both the 9*S* and 9*R* positions. In experiments where the BacA product *en*-H_2HPP was allowed to isomerize nonenzymatically (in solutions estimated at 98% D_2O and then carried through to the BacGF reactions in D_2O), there was very little deuterium at C_9 (Figure S8A of the Supporting Information), perhaps reflecting a large deuterium isotope effect in the nonenzymic isomerization of *en*-H_2HPP solely to the 3*E*-*ex*-H_2HPP isomer. Because of these vagaries due to BacB-mediated exchange and the nonenzymatic isomerization giving solely the 3*E*-*ex*-H_2HPP product,[8] we have not conducted a full interpretation of the C_9 results in the 4*S*-H_4Tyr diastereomer.

■ DISCUSSION

Prephenate is the immediate precursor to both phenylpyruvate (via prephenate dehydratase[16,17]) and hydroxyphenylpyruvate (via prephenate dehydrogenase[18,19]) on the way to L-Phe, L-Tyr, and many phenylpropanoid metabolites.[20,21] In the anticapsin/bacilysin pathway, prephenate is instead shunted down a newly appreciated metabolic branch. BacA, the first enzyme in this and related pathways to dihydro- and tetrahydro-aromatic metabolite scaffolds,[9] is a remarkable catalyst, engineering the decarboxylation without aromatization of the 1,4-cyclohexadiene ring of prephenate.[7] It is a regiospecific isomerization catalyst, working only on the pro-*R*, not the pro-*S*, double bond of the prephenate diene and delivering a proton only to C_6, not $C_{6'}$, a carbon that becomes C_8 in the *en*-H_2HPP product.[8] Three enzymes later, by tandem action of BacBGF, H_4Tyr is formed.

Unlike its familiar aromatic congener L-tyrosine that has one chiral center (2*S*), H_4Tyr has three chiral centers: C_2, the ring junction C_4, and the original alcoholic carbon of prephenate, C_7.

dx.doi.org/10.1021/bi3006362 | *Biochemistry* 2012, 51, 5622−5632

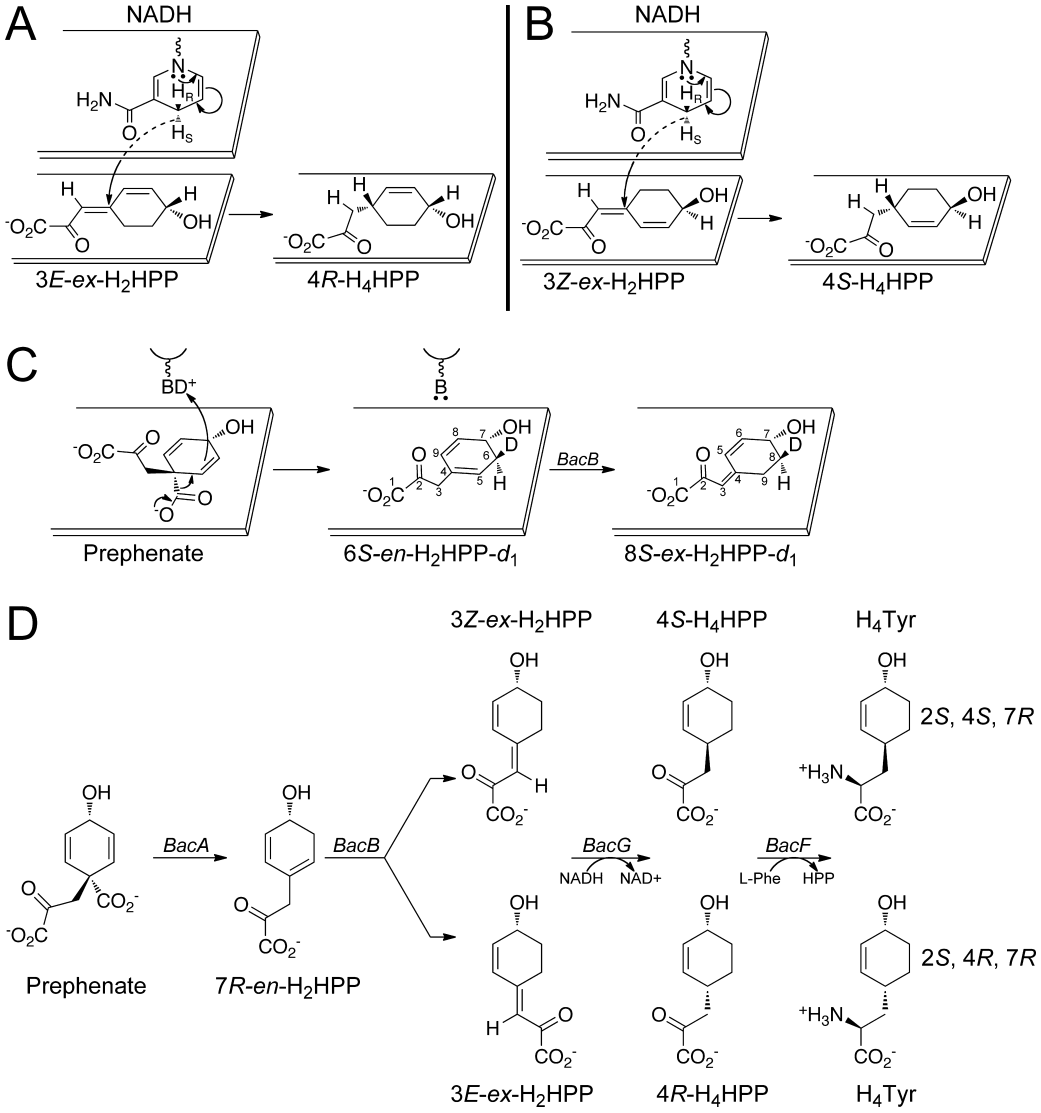

Figure 6. BacG transfers the pro-*S* hydride of NADH to opposite faces of (A) 3*E*-*ex*-H_2HPP and (B) 3*Z*-*ex*-H_2HPP to produce 4*R*-H_4HPP and 4*S*-H_4HPP, respectively. (C) BacA decarboxylation of prephenate performed in D_2O solvent produces *en*-H_2HPP with "*S*" stereochemistry at C_6. This indicates that the incoming proton is delivered to the face of the cyclohexadiene ring opposite the departing CO_2. (D) Action of BacABGF on prephenate produces 2*S*,4*S*,7*R*-H_4Tyr and 2*S*,4*R*,7*R*-H_4Tyr, with the relative amounts produced being determined by the action of BacB.

One expects enzymes to act as chiral catalysts such that of the eight possible H_4Tyr diastereomers, only one is anticipated. The 2*S*,4*S* diastereomer of H_4Tyr is indeed a known nonproteinogenic building block of the cyanobacterial nonribosomal peptides aeruginoside 126A and aeruginoside 126B.[22] In the initial structural assignment of anticapsin, the C_4 stereochemistry was initially incorrectly assigned[1] but corrected subsequent to total synthesis[23] as the 2*S*,4*S* diastereomer, consistent with 2*S*,4*S*-H_4Tyr being on pathway. The stereochemistry at C_7 of anticapsin has become moot because of the oxidation of the C_7 alcohol in prephenate to the ketone in anticapsin. Given that we have recently proven that BacA, by isomerizing the pro-*R* olefin in prephenate, generates the 7*R*-Δ^3,Δ^5-diene, we therefore anticipated the H_4Tyr emerging from tandem action of BacABGF would thus be the 2*S*,4*S*,7*R* diastereomer.

As we have reported here, this expectation is met, but the 2*S*,4*R*,7*R* diastereomer also emerges from the tandem action of the four Bac enzymes. Perhaps most intriguing is the action of the second enzyme, BacB, to generate a mix of 3*Z* and 3*E* isomers of *ex*-H_2HPP. Both are then substrates for conjugate hydride reduction by BacG with delivery of a (pro-*S*) hydride to C_4 and a solvent-derived hydrogen at C_3. At the level of these H_4HPP keto acid products, and after they had been swept through to the more stable H_4-tyrosines via BacF, it is clear that opposite chirality results at C_4. The 3*Z* isomer yields 2*S*,4*S*,7*R*-H_4Tyr from BacG action, while the 3*E* isomer gives 2*S*,4*R*,7*R*-H_4Tyr (Figure 6D). We expect the 4*S* diastereomer is on pathway to anticapsin (4*S*) but not the 4*R* diastereomer. However, this proposition must await study of the last two missing enzymatic steps in anticapsin biogenesis.

The relative orientation of the dihydronicotinamide ring of the hydride donor NADH and the conjugated dienyl keto acid of the *ex*-H_2HPP must switch between the 3*Z* and 3*E* isomers as they are recognized as substrates. If we assume that the NADH orientation stays the same within its BacG binding site, as it transfers the pro-*S* hydrogen to both geometric isomers of substrate, the different faces of the olefin would be presented to the incoming hydride as shown in panels A and B of Figure 6, assuming the C_3−C_1 chain of the geometric *ex*-H_2HPP isomers stays in the same orientation.

dx.doi.org/10.1021/bi3006362 | *Biochemistry* 2012, 51, 5622−5632

The formation of C_4 diastereomers of H_4HPP (and then of H_4Tyr from subsequent BacF action) gives further insight into the possibly corrective role of BacB in the pathway. We have previously noted that the 7*R*-*en*-H_2HPP product of BacA can undergo nonenzymatic conversion to the more conjugated 7*R*-*ex*-H_2HPP isomer. We wondered why the producing cell would expend energy to make a protein (BacB) that would accelerate a reaction that would otherwise occur. Certainly, matching the kinetics of metabolite flux and prevention of off-pathway decomposition and aromatization are reasonable rationales, but most telling is the finding that the nonenzymatic route gives 98% 3*E* geometric isomer. The work reported here shows that the *E* isomer will lead to, via the action of BacG as a reductase, the 4*R* diastereomer of H_4Tyr, which is presumably the wrong chirality to go on to the anticapsin antibiotic. BacB instead equilibrates the more stable 3*E* and less stable 3*Z* geometric isomers to give up to 25% of the 3*Z* isomer, which on subsequent reduction by BacG gives the desired 4*S* stereochemistry. If there is enough BacB in producer cells coupled to the BacG catalytic efficiency preference of 3*Z*/*E* (64/1 found in this study), then flux could be routed selectively to the productive 4*S*-cyclohexenol scaffold. It may be that the 4*R* stereochemistry is useful for one or more alternate downstream metabolites in this or related microbes [i.e., the *diepi* form of 2-carboxy-6-hydroxyoctahydroindole (*diepi*-Choi) (2*R*,4*R* stereochemistry) residues found as constituents of nonribosomal peptides in cyanobacteria].[24]

While a main objective of this study was to ascertain the C_4 stereochemistry from the action of the NADH-utilizing BacG at the stage of reduction of *ex*-H_2HPP to H_4HPP, we have also focused on the stereochemical outcomes at C_8 and C_9 from consecutive action of BacA and BacB in deuterated buffers. While C_8 and C_9 sequentially become CH_2 groups in *en*-H_2HPP and *ex*-H_2HPP, respectively, and the stereochemistry is thus cryptic, in principle the stereochemical course of each enzyme at those carbons could be revealed with deuterium in place of hydrogen. We have previously found[7] that one deuteron from solvent is fixed at C_8 and one at C_9, and in this study, we have shown that BacA introduces the solvent derived (H^+/D^+) from above the plane of the diene in prephenate, yielding 6*S*-*en*-H_2HPP-d_1. Because of the numbering priority changes, this compound becomes 8*S*-*ex*-H_2HPP upon BacB action (Figure 6C). In turn, as gathered from the 4*R*-H_4Tyr result, BacB instead transfers a solvent-derived D^+ from below the plane at C_9 (H_{9a}) and yields a 9*R*-deutero product, swept through to H_4Tyr. (BacB also removes one of the methylene hydrogens at C_3 as it equilibrates the *E* and *Z* geometric isomers of *ex*-H_2HPP.[8]). Interpretation of the ^{1}H−^{1}H NOESY spectrum of protonated 3*E*-*ex*-H_2HPP (Figure S8B of the Supporting Information) established that H_{9a} is on the ring face opposite of H_7.

While it will take structural studies of BacA in complex with substrate and/or product to identify candidate side chains of active site residues such as BH^+, it must be a very efficient process to derail what has been viewed as the default outcome in other members of the prephenate dehydratase superfamily.[16] That default option is cleavage of the C_7−O bond as the cyclohexadiene ring aromatizes, and there has been substantial debate over whether decarboxylation and loss of water is a concerted process.[25,26]

Knowledge of the configuration of the H_4Tyr diastereomers generated by the first four enzymes of the Bac pathway, and the realization that 4*R* and 4*S* products emerge, will provide the appropriate substrates for evaluation and identification of the enzymes responsible for what should be the two remaining steps to obtain the anticapsin warhead: 7*R*-alcohol oxidation and olefin epoxidation.

■ ASSOCIATED CONTENT

Supporting Information

HPLC analysis of *ex*-H_2HPP isomer purity; ^{1}H NMR spectra of 4*R*- and 4*S*-^{2}H-NADH; ^{1}H NMR spectra of H_4HPP isomers synthesized from ^{2}H-NADH; chiral HPLC analysis of BacF-generated tyrosine; additional NMR spectra of deuterated forms of *ex*-H_2HPP, H_4HPP, and H_4Tyr isomers; and tabulated NMR spectral data for H_4HPP and H_4Tyr isomers. This material is available free of charge via the Internet at http://pubs.acs.org.

■ AUTHOR INFORMATION

Corresponding Author

*E-mail: christopher_walsh@hms.harvard.edu. Phone: (617) 432-1715. Fax: (617) 432-0483.

Funding

This work was supported in part by National Institutes of Health Grants AI042738 and GM49338 (C.T.W.).

Notes

The authors declare no competing financial interest.

■ ACKNOWLEDGMENTS

We thank Drs. Sarah A. Mahlstedt, Stuart W. Haynes, Timothy A. Wencewicz, and Steven J. Malcolmson for helpful advice and discussions.

■ ABBREVIATIONS

H_2HPP, dihydro-4-hydroxyphenylpyruvate; H_4HPP, tetrahydro-4-hydroxyphenylpyruvate; H_4Tyr, tetrahydrotyrosine; HPP, 4-hydroxyphenylpyruvate; LC−MS, liquid chromatography−mass spectrometry; NMR, nuclear magnetic resonance; gCOSY, gradient homonuclear correlation spectroscopy; gHSQC, gradient heteronuclear single-quantum coherence; gHMBC, gradient heteronuclear multiple-bond coherence; NOESY, nuclear Overhauser effect spectroscopy; HPLC, high-performance liquid chromatography; D_2O, deuterium oxide; GlcNAc, *N*-acetylglucosamine.

■ REFERENCES

(1) Walker, J., and Abraham, E. (1970) Structure of bacilysin and other products of *Bacillus subtilis*. *Biochem. J. 118*, 563−570.

(2) Milewski, S., Chmara, H., and Borowski, E. (1986) Anticapsin: An active-site directed inhibitor of glucosamine-6-phosphate synthetase from *Candida albicans*. *Drugs Exp. Clin. Res. 12*, 577−583.

(3) Chmara, H. (1985) Inhibition of glucosamine synthase by bacilysin and anticapsin. *J. Gen. Microbiol. 131*, 265−271.

(4) Chmara, H., Zahner, H., and Borowski, E. (1984) Anticapsin, an active-site directed irreversible inhibitor of glucosamine-6-phosphate synthetase from *Escherichia coli*. *J. Antibiot. 37*, 1038−1043.

(5) Steinborn, G., Hajirezaei, M., and Hofemeister, J. (2005) *Bac* genes for recombinant bacilysin and anticapsin production in *Bacillus* host strains. *Arch. Microbiol. 183*, 71−79.

(6) Inaoka, T., Takahashi, K., Ohnishi-Kameyama, M., Yoshida, M., and Ochi, K. (2003) Guanine nucleotides guanosine 5′-diphosphate 3′-diphosphate and GTP co-operatively regulate the production of an antibiotic bacilysin in *Bacillus subtilis*. *J. Biol. Chem. 278*, 2169−2176.

(7) Mahlstedt, S. A., and Walsh, C. T. (2010) Investigation of anticapsin biosynthesis reveals a four-enzyme pathway to tetrahydrotyrosine in *Bacillus subtilis*. *Biochemistry 49*, 912−923.

(8) Parker, J. B., and Walsh, C. T. (2012) Olefin isomerization regiochemistries during tandem action of BacA and BacB on prephenate in bacilysin biosynthesis. *Biochemistry 51*, 3241−3251.

(9) Mahlstedt, S., Fielding, E. N., Moore, B. S., and Walsh, C. T. (2010) Prephenate decarboxylases: A new prephenate-utilizing enzyme family that performs nonaromatizing decarboxylation en route to diverse secondary metabolites. *Biochemistry 49*, 9021−9023.
(10) Horecker, B., and Kornberg, A. (1948) The extinction coefficients of the reduced band of pyridine nucleotides. *J. Biol. Chem. 175*, 385−390.
(11) Gottlieb, H., Kotlyar, V., and Nudelman, A. (1997) NMR chemical shifts of common laboratory solvents as trace impurities. *J. Org. Chem. 62*, 7512−7515.
(12) Viola, R. E., Cook, P. F., and Cleland, W. W. (1979) Stereoselective preparation of deuterated reduced nicotinamide adenine-nucleotides and substrates by enzymatic-synthesis. *Anal. Biochem. 96*, 334−340.
(13) Ottolina, G., Riva, S., Carrea, G., Danieli, B., and Buckmann, A. (1989) Enzymatic-synthesis of [4*R*-H^2]NAD(P)H and [4*S*-H^2]NAD(P)H and determination of the stereospecificity of 7α-hydroxysteroid and 12α-hydroxysteroid dehydrogenase. *Biochim. Biophys. Acta 998*, 173−178.
(14) Mostad, S., and Glasfeld, A. (1993) Using high-field NMR to determine dehydrogenase stereospecificity with respect to NADH: An undergraduate biochemistry lab. *J. Chem. Educ. 70*, 504−506.
(15) Rajavel, M., Mitra, A., and Gopal, B. (2009) Role of *Bacillus subtilis* BacB in the synthesis of bacilysin. *J. Biol. Chem. 284*, 31882−31892.
(16) Kleeb, A. C., Kast, P., and Hilvert, D. (2006) A monofunctional and thermostable prephenate dehydratase from the archaeon *Methanocaldococcus jannaschii*. *Biochemistry 45*, 14101−14110.
(17) Schmit, J. C., and Zalkin, H. (1969) Chorismate mutase-prephenate dehydratase. Partial purification and properties of enzyme from *Salmonella typhimurium*. *Biochemistry 8*, 174−181.
(18) Koch, G. L. E., Shaw, D. C., and Gibson, F. (1970) Tyrosine biosynthesis in *Aerobacter aerogenes*: Purification and properties of chorismate mutase-prephenate dehydrogenase. *Biochim. Biophys. Acta 212*, 375−386.
(19) Hermes, J. D., Tipton, P. A., Fisher, M. A., Oleary, M. H., Morrison, J. F., and Cleland, W. W. (1984) Mechanisms of enzymatic and acid-catalyzed decarboxylations of prephenate. *Biochemistry 23*, 6263−6275.
(20) Vogt, T. (2010) Phenylpropanoid biosynthesis. *Mol. Plant. 3*, 2−20.
(21) Cotton, R., and Gibson, F. (1965) Biosynthesis of phenylalanine and tyrosine: Enzymes converting chorismic acid into prephenic acid and their relationships to prephenate dehydratase and prephenate dehydrogenase. *Biochim. Biophys. Acta 100*, 76−88.
(22) Ishida, K., Christiansen, G., Yoshida, W. Y., Kurmayer, R., Welker, M., Valls, N., Bonjoch, J., Hertweck, C., Boerner, T., Hemscheidt, T., and Dittmann, E. (2007) Biosynthesis and structure of aeruginoside 126A and 126B, cyanobacterial peptide glycosides bearing a 2-carboxy-6-hydroxyoctahydroindole moiety. *Chem. Biol. 14*, 565−576.
(23) Baldwin, J., Adlington, R., and Mitchell, M. (1993) Stereo-controlled enantiospecific synthesis of anticapsin: Revision of the configuration. *J. Chem. Soc., Chem. Commun.,*, 1332−1335.
(24) Lifshits, M., and Carmeli, S. (2012) Metabolites of *Microcystis aeruginosa* bloom material from Lake Kinneret, Israel. *J. Nat. Prod. 75*, 209−219.
(25) Van Vleet, J., Kleeb, A., Kast, P., Hilvert, D., and Cleland, W. W. (2010) ^{13}C isotope effect on the reaction catalyzed by prephenate dehydratase. *Biochim. Biophys. Acta 1804*, 752−754.
(26) Zhang, S., Wilson, D. B., and Ganem, B. (2000) Probing the catalytic mechanism of prephenate dehydratase by site-directed mutagenesis of the *Escherichia coli* P-protein dehydratase domain. *Biochemistry 39*, 4722−4728.